

AD A1157 1:37

AD No.

DDC FILE COPY

HIGH LENGTH-TO-BEAM RATIO SI

**DAVID W. TAYLOR NAVAL SHIP
RESEARCH AND DEVELOPMENT CENTER**

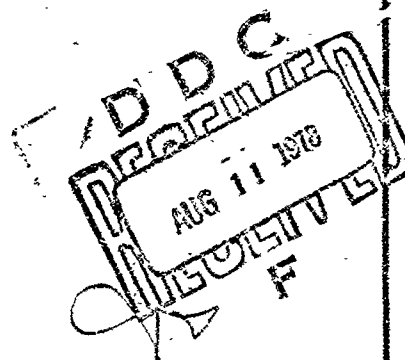
Bethesda, Maryland 20884



HIGH LENGTH-TO-BEAM RATIO SURFACE EFFECT SHIP

by

A.G. Ford
R.N. Wares
W.F. Bush
S.J. Chorney



APPROVED FOR PUBLIC RELEASE: DISTRIBUTION UNLIMITED.

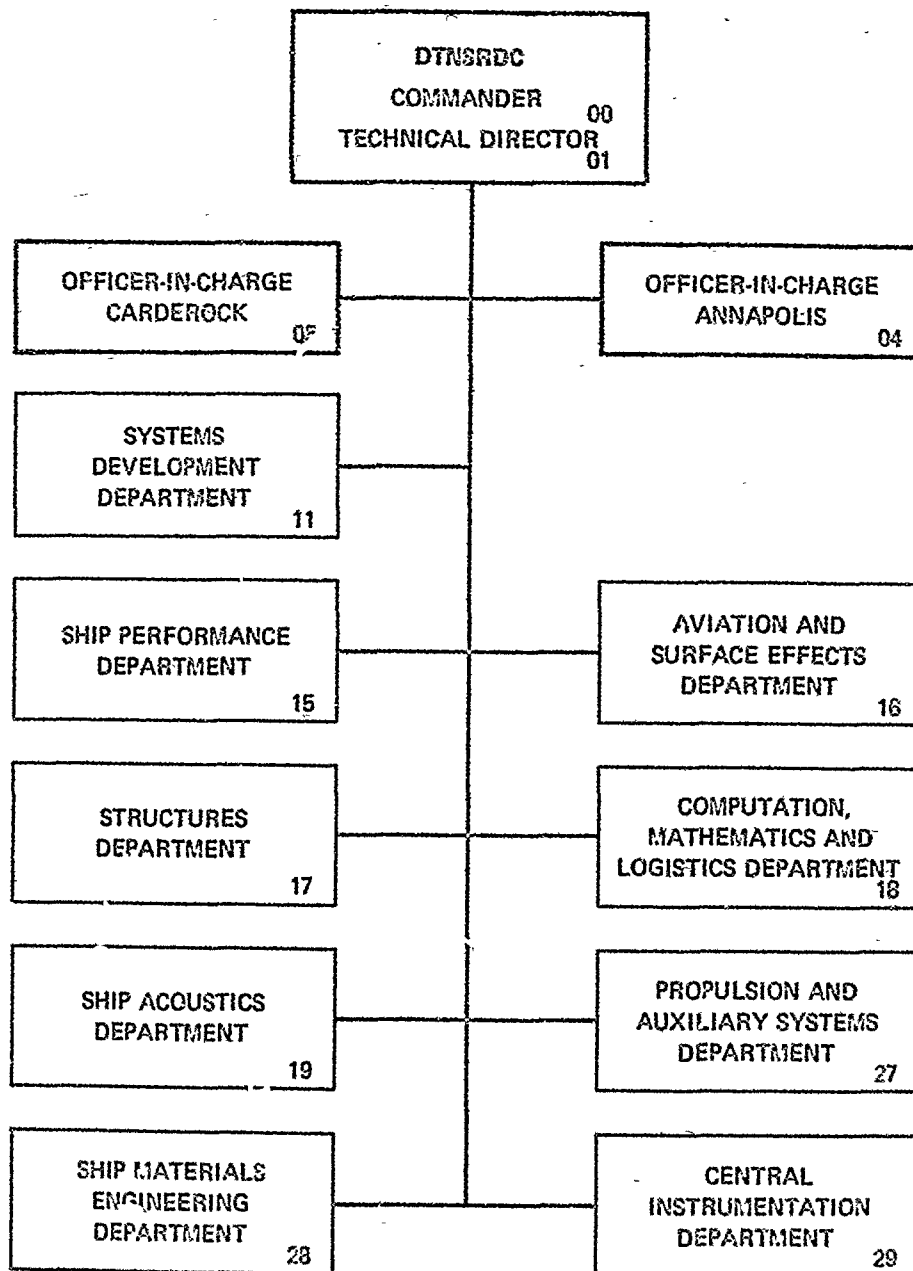
Reprinted from AIAA Paper 78-745

**AVIATION AND SURFACE EFFECTS DEPARTMENT
RESEARCH AND DEVELOPMENT REPORT**

July 1978

DTNSRDC-78/064

MAJOR DTNSRDC ORGANIZATIONAL COMPONENTS



UNCLASSIFIED

SECURITY CLASSIFICATION OF THIS PAGE (When Data Entered)

1. REPORT DOCUMENTATION PAGE		READ INSTRUCTIONS BEFORE COMPLETING FORM
18 1. REPORT NUMBER DTNSRDC 78/064	2. GOVT ACCESSION NO.	3. RECIPIENT'S CATALOG NUMBER
6 4. TITLE (and Subtitle) HIGH LENGTH-TO-BEAM RATIO SURFACE EFFECT SHIP,	5. TYPE OF REPORT & PERIOD COVERED	
10 7. AUTHOR(s) A. G./Ford, R. N./Wares, W. F./Bush S. J./Chorney	6. PERFORMING ORG. REPORT NUMBER Aero Report-1251 CONTRACT OR GRANT NUMBER(s)	
9. PERFORMING ORGANIZATION NAME AND ADDRESS David W. Taylor Naval Ship R&D Center Aviation and Surface Effects Department Bethesda, Maryland 20084	10. PROGRAM ELEMENT, PROJECT, TASK AREA & WORK UNIT NUMBERS (See reverse side)	
11. CONTROLLING OFFICE NAME AND ADDRESS Naval Sea Systems Command Surface Effect Ships Project Office (PMS-304) Bethesda, Maryland 20084	12. REPORT DATE July 1978	13. NUMBER OF PAGES 22
14. MONITORING AGENCY NAME & ADDRESS (if different from Controlling Office)	15. SECURITY CLASS. (of this report) UNCLASSIFIED 12/22/01	
15a. DECLASSIFICATION/DOWNGRADING SCHEDULE		
16. DISTRIBUTION STATEMENT (of this Report) APPROVED FOR PUBLIC RELEASE: DISTRIBUTION UNLIMITED		
17. DISTRIBUTION STATEMENT (of the abstract entered in Block 20, if different from Report)		
18. SUPPLEMENTARY NOTES Presented at the AIAA/SNAME Advanced Marine Vehicles Conference, San Diego, California, 17-19 April 1978. AIAA Paper No. 78-745.		
19. KEY WORDS (Continue on reverse side if necessary and identify by block number) Surface Effect Ship High Length-to-Beam Drag Prediction Parameters		
20. ABSTRACT (Continue on reverse side if necessary and identify by block number) Experimental and predicted results are presented in the areas of drag and powering, motions and maneuvering and control for High Length-to-Beam (L/B) Surface Effect Ships (SES). The High L/B SES designs offer lower total drags than the Low L/B SES up to a crossover speed. The crossover speeds increase with displacement. For displacements above about 5000 tons, design speeds as high as 60 knots are reasonable values. Results are given (Continued on reverse side)		

DD FORM 1 JAN 73 1473

EDITION OF 1 NOV 65 IS OBSOLETE
S/N 0102-LF-014-6601

UNCLASSIFIED

SECURITY CLASSIFICATION OF THIS PAGE (When Data Entered)

387 075

Lee

UNCLASSIFIED

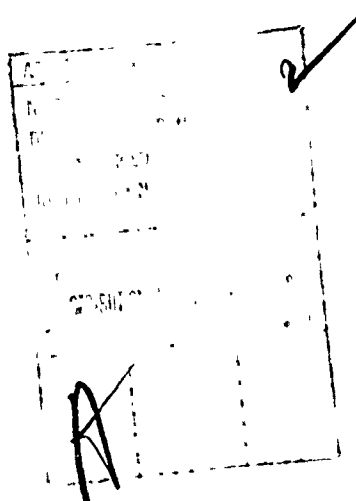
SECURITY CLASSIFICATION OF THIS PAGE (When Data Entered)

(Block 10)

Task Area SO 308 001
Program Element 63534N
Work Unit 1-1630-050

(Block 20 continued)

which indicate that High L/B SES designs have excellent potential for achieving transoceanic and greater ranges and are particularly applicable to displacements of 5000 tons and greater.



UNCLASSIFIED

SECURITY CLASSIFICATION OF THIS PAGE (When Data Entered)

TABLE OF CONTENTS

	Page
LIST OF FIGURES	iii
TABLE	v
ABSTRACT.	1
INTRODUCTION.	1
DRAG AND POWERING	1
EXPERIMENTAL PROGRAM.	3
PARAMETRIC CONSIDERATIONS	7
SUMMARY	15
REFERENCES.	15

LIST OF FIGURES

1 - High Length-to-Beam Surface Effect Ship Artist Concept. . .	1
2 - Vector Representation of Wavemaking Drag.	2
3 - Wave Drag Parameter Based on Length versus Froude Number Based on Length	2
4 - Wave Drag Parameter Based on $A^{1/2}$ versus Froude Number Based on $A^{1/2}$	2
5 - Total Drag as a Function of Velocity and Length-to-Beam Ratio	2
6 - Crossover Speed for L/B 2.0 and 6.0 as a Function of Displacement ($w/A^{1/2} = 2$)	3
7 - High L/B SES Model.	4
8 - High L/B SES Model During High-Speed Test	4
9 - High L/B SES Testcraft (XR-5) During Construction	4
10 - XR-5 Testcraft During Performance Trials.	4
11 - XR-5 Testcraft Operating With Chase Boat.	4

	Page
12 - A Variable L/B SES Model (In L/B 4.0 Configuration) During Calm Water Performance Experiments.	5
13 - Model Drag-to-Weight versus $F_A^{1/2}$ and Scale Velocity	5
14 - Model Drag versus Velocity as a Function of Flow Rate. . . .	5
15 - Weight Variation Predictions -- Parametrics versus Model Data.	6
16 - Length-to-Beam Ratio Variation Predictions -- Parametrics versus Model Data.	6
17 - Sea State Variation Predictions -- Parametrics versus Model Data.	6
18 - Theodolite Tracking Plot of XR-5 Manned Craft.	7
19 - XR-5 and DD-931 Turn Diameter Comparison	7
20 - Heave Acceleration versus Velocity for L/B 3.0 and 5.0 SES.	7
21 - Comparison of Scaled Ship Motions.	7
22 - Drag versus Velocity for Four Displacements and Four L/B Values.	9
23 - Power versus Velocity for Four Displacements and Four L/B Values.	10
24 - Performance Plot Showing Speed Capability for Various Fuel Loadings as a Function of Thrust.	11
25 - Sea State Degradation for an 8,000 ton, L/B 6.0 SES.	11
26 - Total Drag versus Velocity Comparison for L/B 2.0 and 6.0.	11
27 - Effective Horsepower versus Velocity for L/B 2.0 and 6.0.	12
28 - Propulsive Horsepower Requirements for L/B 2.0 and 6.0 8,000 Ton SES Compared with Conventional Displacement Ships	12
29 - Range versus Velocity as a Function of L/B	12
30 - Propulsive Shaft Horsepower per Ton versus Velocity for a High L/B SES.	13

	Page
31 - Transport Efficiency versus Velocity for L/B 2.0 and 6.0	13
32 - Lift-to-Drag Ratio for L/B 2.0 and 6.0	13
33 - Fuel Burn Rate versus Velocity for L/B 2.0 and 6.0	13
34 - Total Horsepower versus Velocity Illustrating SES Design Options.	14

Table 1 - SES Powering Characteristics.	14
---	----

HIGH LENGTH-TO-BEAM RATIO SURFACE EFFECT SHIP

A. G. Ford, Head, SES Division
R. N. Wares, Aerospace Engineer
W. F. Bush, Lt., USN, Surface Effects Program Officer
S. J. Chorney, Aerospace Engineer

Aviation and Surface Effects Department
David W. Taylor Naval Ship Research and Development Center
Bethesda, Maryland 20084

Abstract

Experimental and predicted results are presented in the areas of drag and powering, motions and maneuvering and control for High Length-to-Beam (L/B) Surface Effect Ships (SES). The High L/B SES designs offer lower total drags than the Low L/B SES up to a crossover speed. The crossover speeds increase with displacement. For displacements above about 5000 tons, design speeds as high as 60 knots are reasonable values. Results are given which indicate that High L/B SES designs have excellent potential for achieving transoceanic and greater ranges and are particularly applicable to displacements of 5000 tons and greater.

Introduction

There are a number of articles describing the rationale and history of surface effect ships (SES's),^{1,2,3} so that task will not be attempted here. What will be attempted is to describe the high length-to-beam ratio SES and to show its place in the design spectrum of all SES's.

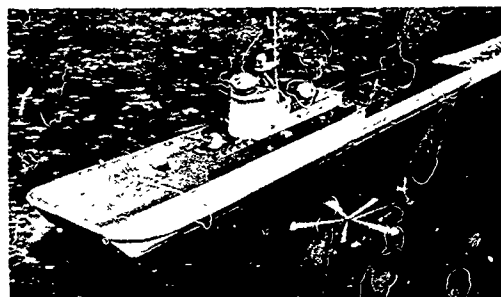
The first obvious question to answer is: What constitutes a high length-to-beam ratio (or High L/B) SES? Fig. 1 contains an artist's conception and three views of such a ship. The essential elements of any SES are present. A pressurized region or an air cushion lifts the SES and reacts against the water below. Fans (not shown) pump air from atmospheric pressure to cushion pressure. Separate fans also deliver air to end-seal bags at slightly higher than cushion pressure; this air then flows from the seal bags into the cushion. The sidewalls and fore and aft seals prevent cushion air leakage except in the lower extremities. Thus the lower region of the air cushion tends to act as a near frictionless surface, and the seals, being flexible, have a capability of moving up and down in response to a wave. The sidewall shape in its lower outboard region is such that stabilizing (roll-in) moments can be generated in a turn.

However, these are the essential elements and components of any SES. Therefore, the High L/B SES differs from other SES's only in the respect that the ratio of its length to its beam is large (e.g., 5 to 7). It will become clearer later whether this is advantageous, and if so, under what design conditions. The artist's concept in Fig. 1 shows a multi-thousand-ton, High L/B SES as a helicopter carrier performing some appropriate Navy mission.

Drag and Powering

In order to understand the appropriate design region of the High L/B SES, it is necessary to understand the nature of wavemaking drag of an SES in calm water, because it plays a significant role in determining the total SES drag, and hence the thrust required to overcome it.

Copyright © American Institute of Aeronautics and Astronautics, Inc., 1978. All rights reserved.
Reproduced with permission.



HIGH LENGTH-TO-BEAM RATIO
SURFACE EFFECT SHIP

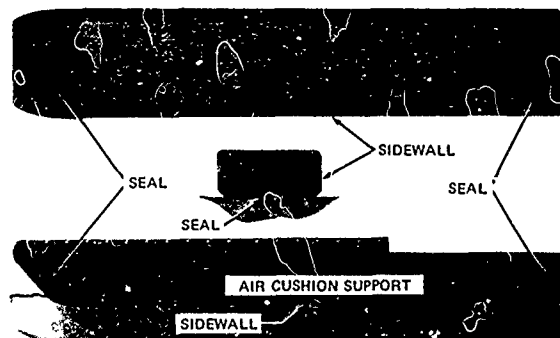


Fig. 1 - High Length-to-Beam Surface Effect Ship
Artist Concept

The appropriate hydrodynamic situation is illustrated in Fig. 2. When an SES is at higher speeds in calm water, the inside water line tilts down by some angle α as a reaction to cushion pressure. A long wave is then generated aft of the SES; hence the name "wavemaking drag" or "wave drag." Thus the resultant force R that the cushion exerts (generally upward) tilts aft of vertical by the angle α . Hence, R can be broken into a vertical or lift component L , and a horizontally directed wavemaking-drag component D_w . It is this wavemaking drag D_w (with other drag components) that must be counteracted by a propulsion system thrust in order to sustain the SES at constant speed.

Fig. 3 illustrates one standard method of presenting wavemaking drag.^{4,5} On the ordinate the wavemaking drag/lift ratio D_w/L is further normalized by the cushion pressure-to-length ratio

p/ρ_c ; the abscissa is the Froude number F_L based on cushion length. There are some difficulties with using this figure to establish comparisons of the wavemaking drags of SES of differing length-to-beam ratios; these will be explained shortly.

Fig. 4 presents the same basic drag information but on a modified axis system. In this case the wavemaking drag-to-lift ratio D_w/L on the ordinate is normalized by the specific loading parameter $w/A^{1/2}$; also, the abscissa is the Froude number based on the square root of the cushion area. Fig. 4 is more useful than Fig. 3 in forming a mental comparison of the SES's wavemaking drags for differing length-to-beam ratios. For example, comparing the wavemaking drags of two SES's with different L/B , but the same displacement (or gross weight), and having the same cushion area and pressure, then, at the same ship speed, these values can be read at one value of Froude number in Fig. 4. This is not true of Fig. 3, because the cushion length ℓ_c in the abscissa varies with L/B when the cushion area is held constant. Further, in Fig. 4, the ordinate values are proportional to the wavemaking drags. Again, this is not true of Fig. 3, for the same reason given above.

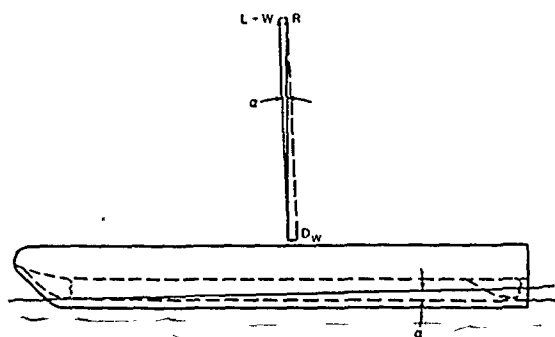


Fig. 2 - Vector Representation of Wavemaking Drag

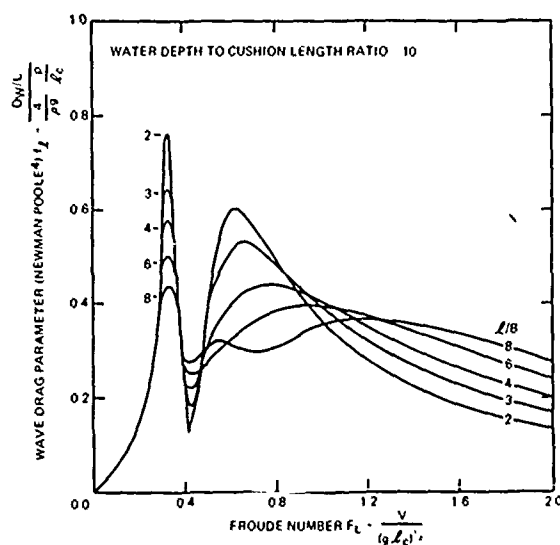


Fig. 3 - Wave Drag Parameter Based on Length versus Froude Number Based on Length

The conclusion that can be drawn from Fig. 4 is that, for SES of higher L/B , the wavemaking drags are generally substantially lower than those of lower L/B , except at the very high Froude numbers.

Fig. 5 shows a plot of total drag versus velocity of several SES's with different L/B values, but the same displacement W and cushion area A . The ratio W/A (or w) is approximately equal to cushion pressure p because of the small buoyancy lift contribution of the SES sidewalls and seals. The general shapes of the curves of Fig. 5 are expected -- having seen Fig. 4. At the lower

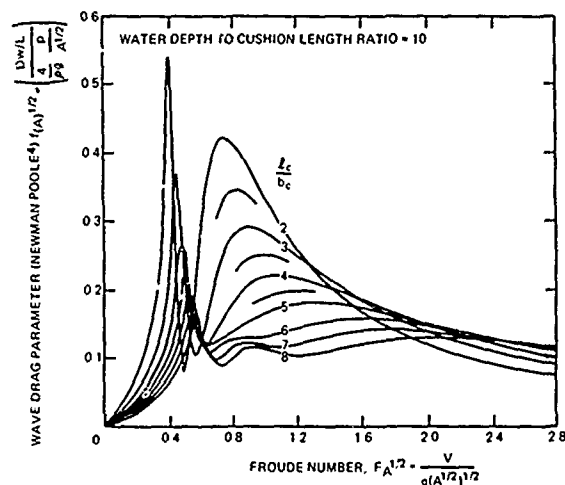


Fig. 4 - Wave Drag Parameter Based on $A^{1/2}$ versus Froude Number Based on $A^{1/2}$

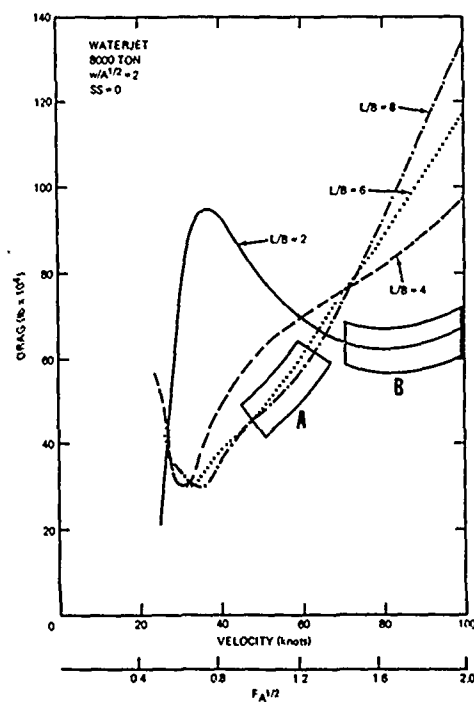


Fig. 5 - Total Drag as a Function of Velocity and Length-to-Beam Ratio

speeds the wavemaking drag D_w from Fig. 4 predominates. At higher speeds, however, the sidewall and seal skin friction drags become important. For higher values of L/B , the sidewalls are longer; hence, the drag rises more steeply with speed.

Fig. 5 is generated by a theoretically-based SES Parametrics Design computer program. It is not the intent here to describe the drag and powering portions of this program in any great detail. However, it has been shown to correlate well with experimentally measured SES drags. This will be discussed later in greater detail.

The conclusions that can be drawn from Fig. 5 are as follows:

1. Region A is the natural design speed regime of a High L/B SES.
2. Region B is the natural design speed regime for the Low L/B SES.

These conclusions are based on the fact that, in each region, the SES with that L/B has the lowest total drag. Comparing design Regions A and B, B has the advantage of having the higher speed, but it also has the higher drag (compared to A) and the more pronounced drag hump at a speed between 30 to 40 knots. Region A has a lower but still appreciable speed, a lower drag (compared to B), and a less pronounced drag hump below 30 knots (see Fig. 4). The advantage of a low drag hump is that with increased ship design weight, or increased wave height, only small velocity degradations will occur, without incurring an inability to transit the hump region.

In an overall view of SES design Regions A and B, it can be concluded that the SES principle applies very broadly; that is, it applies not only to ships of very high speed (B), but also to ships of moderately high speed (A).

Intermediate values of L/B (e.g., $L/B = 4$) do achieve substantial reductions in hump drag, but at the price of increased drag at high speed. At no speed do they appear to have the lowest drag.

The intersection of Regions A and B occurs at a speed that can be referred to as the crossover speed. This crossover speed serves as an indicator of the speed above which an SES design would appropriately be low L/B , and below which it would appropriately be high L/B .

Fig. 6 is a plot of this crossover speed (the intersection of $L/B = 2$ and $L/B = 6$) as a function of SES displacement. These crossover speeds vary from about 52 knots at 2,000 tons* to about: 60 knots at 5,000 tons, 68 knots at 10,000 tons, and 77 knots at 20,000 tons.

The conclusion that can be drawn from this figure is that, in larger SES (e.g., 5,000 to 10,000 tons), relatively high speeds are realizable for high L/B designs on an efficient design basis.

*Tons refers to long tons.

**Under sponsorship of the Independent Exploratory Development (IED) program at DTNSRDC.

Also it is at these large displacements that limiting the magnitude of the installed power becomes important, even though the desire for still higher speed is legitimately present. For these reasons, the high L/B designs are considered to be most applicable to the larger SES displacements (e.g., 5,000 to 10,000 tons and beyond) for Navy missions where large payloads are required. In general, for a high L/B design, the crossover speed will be the maximum speed, unless an additional dash speed is required and designed for. However, maximum speeds of less than crossover speed are effective in limiting the maximum installed power, and are also available as design points.

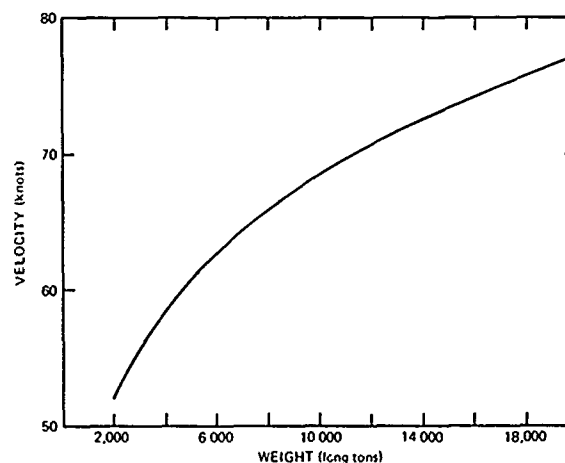


Fig. 6 - Crossover Speed for $L/B = 2.0$ and 6.0 as a Function of Displacement ($w/A^{1/2} = 2$)

Experimental Program

Realizing the potential of the High L/B SES, an exploratory development program was initiated at the David W. Taylor Naval Ship Research and Development Center (DTNSRDC) in the early 1970's.** Fig. 7 shows the High L/B SES model ready for drag and powering tests. The picture is taken from below and forward of the 15-ft long model. The sidewalls, fore and aft seals, and the fan entrance areas to the cushion can be seen.

Fig. 8 shows this same model at high speed in a test in a towing tank. The scale speed of the model in Fig. 8, as a 5000-ton SES, is 80 knots. In spite of this very high speed (above the crossover speed), the wake pattern is very small; it can be seen just aft of the forward intersection of the sidewall with the water surface. In this multiyear DTNSRDC program, powering and motion tests were performed with various seal designs in calm water and seas; also stability tests and analyses were conducted.

The foregoing effort was sufficiently successful that it was decided to proceed with construction of a free-running, manned model. Fig. 9 shows the manned experimental SES craft, the XR-5, under construction** in the DTNSRDC shops. The XR-5

overall length is 47 ft (its beam is 8 ft), with a cushion length-to-beam ratio of 6.5. The frame is aluminum and the craft is covered with plywood and fiberglass. Its operating weight is about 4 tons. It is powered by two 55 hp outboard engines mounted through direct measuring thrust block gages. Six fans powered by a 30 hp electric generator, deliver cushion air at approximately 28 lb/ft².

Fig. 10 shows the XR-5 in operation at the SES Test Facility, Patuxent River, Maryland.* Its maximum speed is about 25 knots (83 knots for a 5000-ton SES); this extends beyond the Froude range of interest.

In Fig. 11, the XR-5 is operating with a chase boat, and the wake patterns of both craft can be seen. The chase boat weight is about two-thirds that of the XR-5, and it is utilizing about twice the power. This power and weight comparison is consistent with the fact that the chase boat has a much larger wake pattern, even though the speeds are the same.

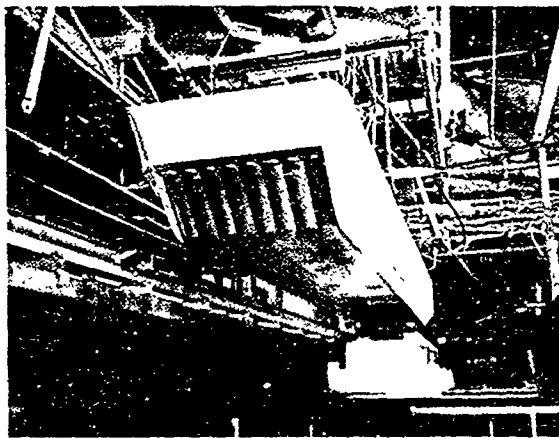


Fig. 7 - High L/B SES Model

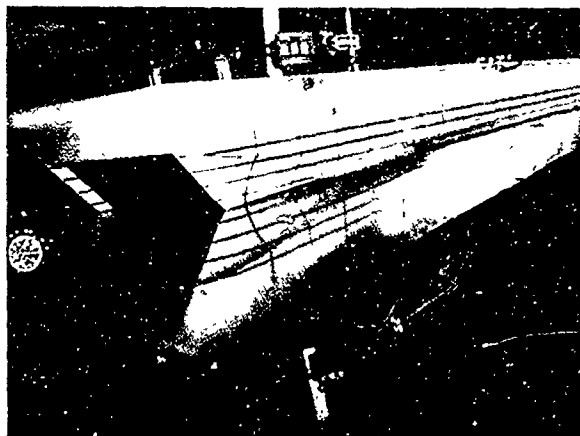


Fig. 8 - High L/B SES Model During High-Speed Test

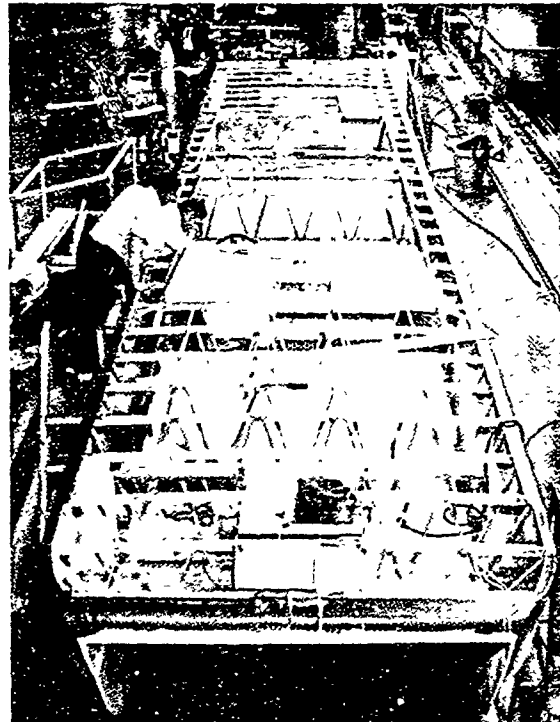


Fig. 9 - High L/B SES Testcraft (XR-5) During Construction

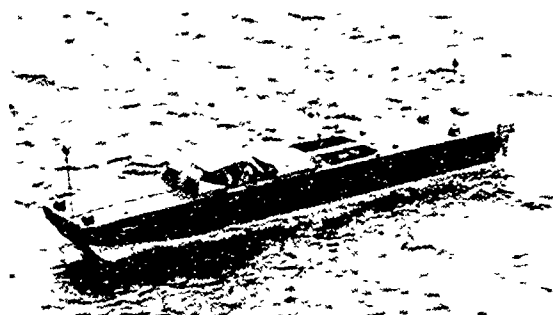


Fig. 10 - XR-5 Testcraft During Performance Trials



Fig. 11 - XR-5 Testcraft Operating With Chase Boat

*This test and evaluation phase was jointly financed by DTNSRDC (IED) and the SES Project Office (PMS-304).

During FY74, the XR-5 underwent trials during which drag, motions, and maneuvering data were taken. The following year, an extensive update and improvement of the XR-5 data acquisition system was accomplished, and more extensive trials (including structural tests in waves) were done utilizing the new instruments. These trials demonstrated the operational feasibility and capability of the High L/B SES.

Additional verification of the performance potential of higher length-to-beam SES vehicles was made possible by the "Various Length-to-Beam SES Design" experimental studies. This project was initiated in 1976 and funded by both the SES Project Office (PMS-304) and the Advanced Naval Vehicle Concept Evaluation (ANVCE) program office. These experiments have generated a wealth of powering performance model data for correlation with the existing SES parametrics prediction program as well as for the assessment of SES vehicles having L/B ratios greater than the previously nominal range of 2.0 to 2.3. Prior to these tests, little or no SES model performance data existed in the mid-L/B ranges between 2.4 to 6.5.

Fig. 12 is a photograph of one of the models during calm-water powering tests on Carriage III, at DTNSRDC. In this series of tests, SES designs over a range of L/B values from 2.4 to 6.5 were evaluated. Two classes of full-length sidewall design were incorporated, and the performance of all models was examined over a wide range of specific loading parameter $w/A^{1/2}$, flow rates, and LCG positions -- in both calm water and scaled seas. In addition, various seal designs were examined with an L/B 5.0 model.

Some typical experimental results are shown in Figs. 13 and 14. Fig. 13 contains two curves of the unscaled model drag-to-weight ratio D/W versus $F_A^{1/2}$ and scale velocity (for a 5600-ton SES). One plot is for L/B 2.4 and one for L/B 5.0, but each has the same specific loading parameter $w/A^{1/2}$. As the L/B increases from 2.4 to 5.0, significant decreases in D/W occur in the secondary hump and medium speed regime, until a crossover is reached at approximately a Froude number $F_A^{1/2} = 1.37$ (63 knots full-scale). Beyond the crossover speed, the model D/W increases as the L/B increases from 2.4 to 5.0.

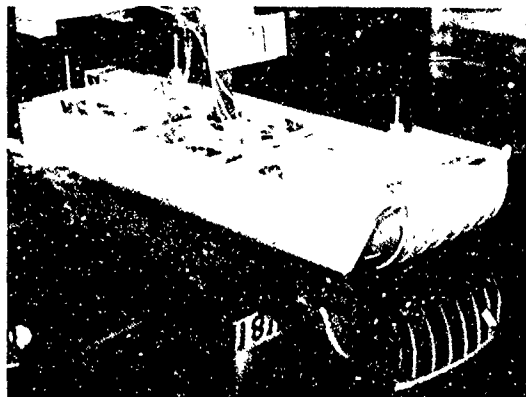


Fig. 12 - A Variable L/B SES Model (In L/B 4.0 Configuration) During Calm Water Performance Experiments

Typical performance results as a function of velocity and lift-fan flow rates are plotted in Fig. 14 for the L/B 5.0 model. It is seen that, in the secondary-hump regime and beyond (to a velocity of about 15 ft/s), large variations in flow rate have little, if any, effect on drag. Only at high model speeds (16 ft/s or approximately 60 knots full-scale and beyond) do the higher flow rates result in significant drag reductions.

As mentioned previously, a primary reason for this experimental SES work was to provide a data

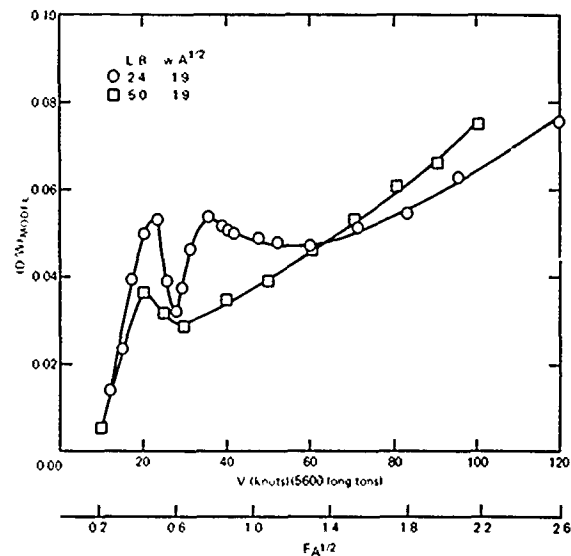


Fig. 13 - Model Drag-to-Weight versus $F_A^{1/2}$ and Scale Velocity

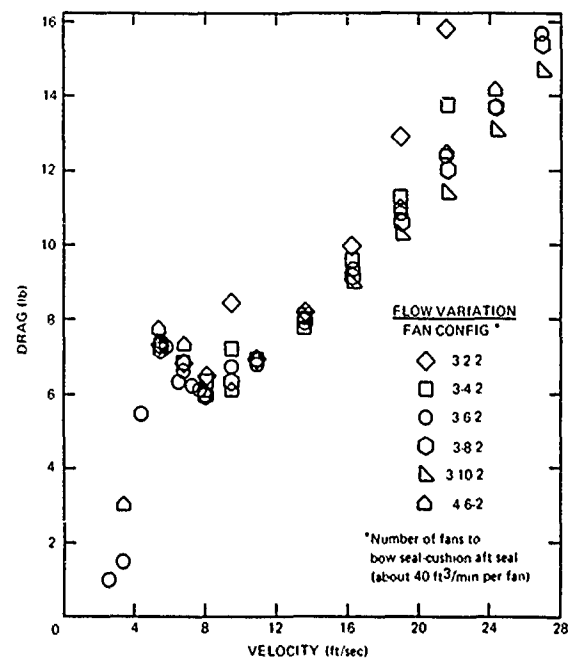


Fig. 14 - Model Drag versus Velocity as a Function of Flow Rate

base for correlation with existing predictive techniques, particularly the SES parametrics computer program. This program (discussed in more detail later) has served as a useful tool in predicting drag as well as other characteristics of various size SES vehicles. The model results have, for the most part, confirmed the powering predictions of the program and are currently being utilized to further update and improve them.

The next three figures present comparisons of model results with predictions from the SES parametrics design program. Plots of L/B 5.0 model drag as a function of velocity and specific loading parameter are shown in Fig. 15 and compared with these predictions. The experimental drag results at high speed (above about 10 ft/s) are in good agreement with the predictions for all values of velocity and the specific loading parameter $w/A^{1/2}$. The experimental drag results in the secondary hump regime (5 to 10 ft/s) are higher than estimated. But it should be noted that during these tests, the bow and stern seal trailing edges were set at the sidewall keel level. Investigations have shown that raising the planing seals in this speed regime reduces drag closer to the values predicted.

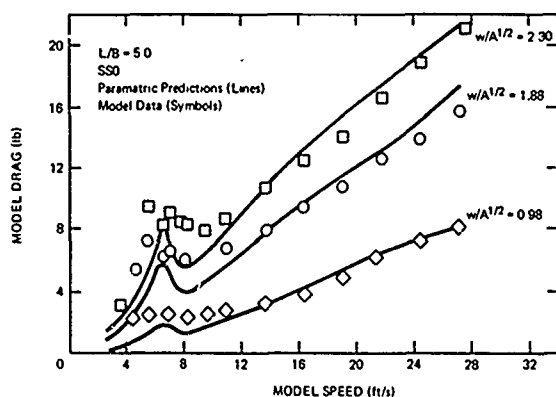


Fig. 15 - Weight Variation Predictions -- Parametrics versus Model Data

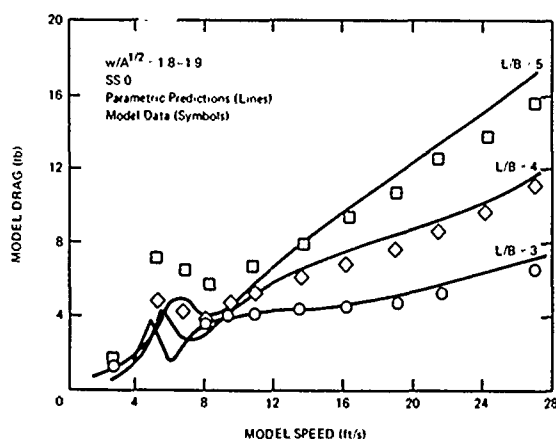


Fig. 16 - Length-to-Beam Ratio Variation Predictions -- Parametrics versus Model Data

Comparisons of drag predictions with model data, for a broad speed range and for several L/B values, are plotted in Fig. 16. The model specific loading parameter $w/A^{1/2}$ and lift fan configurations are identical for each length-to-beam ratio. Again the trends show a high degree of correlation between predicted and experimental results in the design range of interest. It should be noted that in the L/B 5.0 case, 24 ft/s corresponds to a full-scale velocity of approximately 90 knots for a 6000-ton SES.

Fig. 17 gives examples of performance comparisons between high L/B model data and the parametrics program over a range of experimental sea conditions. The results presented for a L/B 5.0 configuration are at a constant speed of 13.6 ft/s (50 knots full-scale). The plots indicate that a high degree of correlation exists at operational speeds from calm water to a State 5 sea. Only at very high sea conditions does the model drag begin to diverge from that predicted. The large data base resulting from these experiments is at present being utilized to incorporate further refinements in the prediction of sea state degradation. In most circumstances of design interest, however, satisfactory correlation already exists.

Stability and control characteristics of high length-to-beam SES configurations have also received a good deal of attention. Stability considerations were of utmost importance during the development and subsequent trials of the XR-5 manned craft. At that time a five-degree-of-freedom (5-DOF) data-based maneuvering and control simulation program was developed at DTNSRDC. This simulation routine, in conjunction with model tests, provided a high degree of confidence in the stability characteristics of the XR-5 craft prior to the actual trials.

Stability envelopes were developed and expanded during these two years of trials through the use of an onboard data acquisition system in conjunction with a theodolite tracking system. A theodolite tracking XY plot of the XR-5 during a

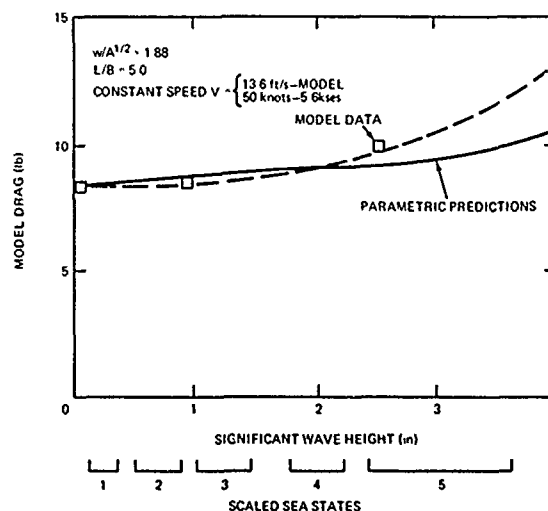


Fig. 17 - Sea State Variation Predictions -- Parametrics versus Model Data

typical maneuver is presented in Fig. 18. Under all circumstances the XR-5 proved to be highly stable and maneuverable. Fig. 19 shows an example of the turn-diameter-to-length ratio versus Froude number for the XR-5 and (for comparison) for a typical destroyer. In general the 5-DOF simulation verified the results of the trials.

A prime objective of the recent "Various L/B SES Design" program has been to provide an improved and expanded data base for utilization in the 5-DOF simulation. Extensive stability tests were performed with an L/B 5.0 model in order to obtain static stability information as well as dynamic coefficients; the latter information was obtained in lateral-planar-motion-mechanism (LPMH) experiments. The effects of various size appendages were examined in addition to bare hull characteristics. These data are presently being incorporated into the 5-DOF program. This program will be utilized to parametrically size appendages for various SES designs, thus, the resultant designs will provide adequate ship stability and safety. These rudder (or fin) designs will then be used in the SES drag and powering prediction program.

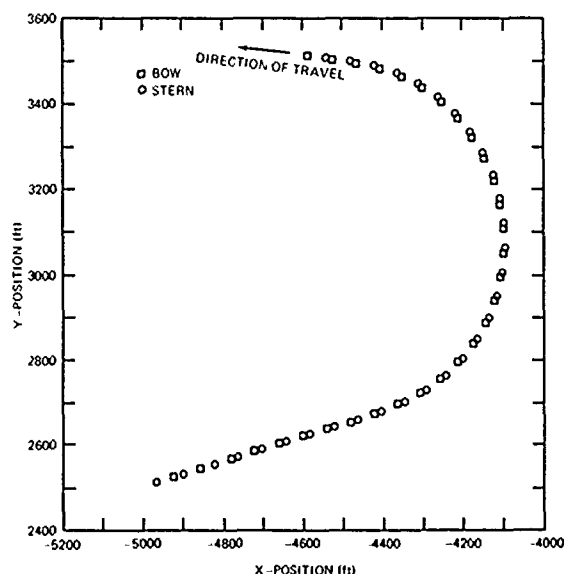


Fig. 18 - Theodolite Tracking Plot of XR-5 Manned Craft

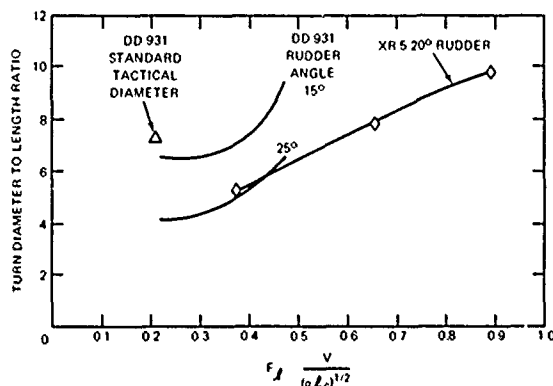


Fig. 19 - XR-5 and DD-931 Turn Diameter Comparison

Mention should also be made of motions information obtained during the model sea state performance experiments. This information has given an additional indication of the acceptability of high L/B designs as stable platforms. Fig. 20 presents plots of heave acceleration versus velocity for the L/B 3.0 and 5.0 configurations. It is clear that the motions of the high L/B design are, as one would expect, equally good, if not better, than the lower L/B design. Further evidence of the acceptability of the SES platform characteristics is given in Fig. 21 where L/B 5.0 scaled data are compared with those of a scaled similar size displacement ship; in this case a 5600-ton frigate.

Parametric Considerations

The subsequent sections of this paper are designed to show how the application of parametric analysis techniques supports conceptual design studies of high performance ships. Parametric analysis is a very valuable tool in the beginning stages of ship design. The ability to look at a large number of interacting variables simultaneously is an asset in any phase of ship design or in any sizing study. However, the primary use of parametric analysis in the context of this paper is to allow those involved in conceptual ship

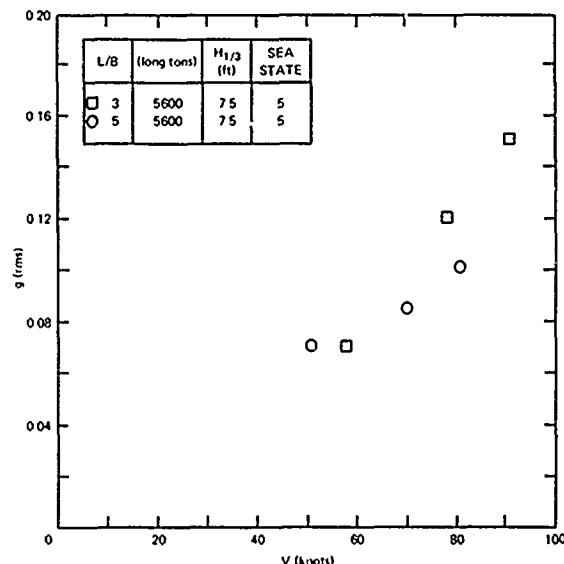


Fig. 20 - Heave Acceleration versus Velocity for L/B 3.0 and 5.0 SES

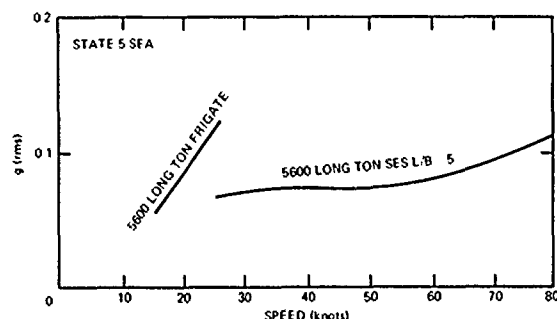


Fig. 21 - Comparison of Scaled Ship Motions

design the ability to arrive at a realistic, initial, design point. This can best be done by displaying the necessary variables so that the optimum choice becomes easier to identify.

The results of any parametric exploration of multidimensional space is only as good as the theoretical relationships employed. The SES Parametrics Computer Prediction Program at DTNSRDC is the primary tool used in SES sizing studies to date. One of its principal uses is in determining the drag and powering requirements once the displacement and cushion geometry are given. Data for large families of ships can thus be generated. Examples follow.

Fig. 22 consists of multiple plots of drag versus velocity for displacements of 6,000, 8,000, 10,000, and 12,000 tons. Each plot contains four curves of drag versus velocity, one for each value of L/B (2, 4, 6, and 8). The net result of Fig. 22 is to graphically portray drag variations with velocity, length-to-beam ratio, and SES displacement.

Fig. 23 consists of multiple plots of propulsive power versus velocity, one plot for each of four SES displacements (6,000, 8,000, 10,000, and 12,000 tons). Each plot contains four curves of propulsive power versus velocity, one for each value of L/B (2, 4, 6, and 8). Figure 23 displays propulsive power variations with velocity, length-to-beam ratio, and SES displacement.

Figs. 22 and 23 show one type of result from the SES Parametrics Computer Prediction Program. They clearly show the crossover speeds for each weight category and for the various L/B pairs. This relationship of the crossover speed versus displacement for the L/B 2 and 6 combination was introduced earlier as Fig. 6. Figs. 22 and 23 are also of much interest because of their value in making gross propulsive power requirement estimates as displacement and geometry become relatively fixed in the design selection process.

The SES Parametrics Computer Prediction Program is considered a valid tool for the following reasons: (1) It correlates well with the bank of model data available. (2) It correlates well with SES prototype data determined from model data scaled by the "SES Scaling Program." (3) It correlates well with optimum SES 100-ton testcraft data and other testcraft data. The assumption here is that if the program correlates well with (1), (2), and (3) from above, then it should also correlate well with full-scale (prototype) data. If doubt exists in the above correlations, then at least an argument can be made for the trends of the output data.

Since some design requirements exist in the form of operational needs, such as a certain speed capability in a given sea state, attainment of minimum range, adequate thrust margin, etc., it is possible

to address these types of requirements with a program which produces performance characteristics as a function of velocity.

The parametrics prediction program that is referred to in this paper is the SES Parametrics Computer Prediction Program, SESPAR.* It utilizes a theoretical approach to drag and power prediction which is modified where required by semiempirical results from extensive experience with model and testcraft data. SESPAR contains several subroutines in addition to the basic program. Four major subroutines related to performance are SESRES, LIFT, SPLASH (or SQUIRT), and RANGE.

1. SESRES contains detailed expressions for the calculation of component drags. In this subroutine wavemaking drag is basically calculated by using the wavemaking drag theory of Ref. 4 modified by an empirical curve fit in the secondary subhump region to eliminate tertiary and higher order humps which do not appear experimentally.**

2. LIFT is a subroutine for calculating lift power requirements. The expression, based on experimental results for minimum power requirements, predicts airflow rates at the required cushion pressure.

3. SPLASH or SQUIRT are subroutines for the calculation of the net propulsive coefficient (NPC) for either a semisubmerged supercavitating propeller (SSSC) or a waterjet. The NPC is defined as the product of the net propulsor thrust and the ship's velocity divided by the product of the transmission efficiency and the power at the output shaft of the prime mover. Peak values of NPC considered to be achievable in the future are approximately 0.55 for waterjet and 0.68 for the SSSC propeller. This estimate is, in itself, an important conclusion which shows the SSSC propeller NPC to be about 25 percent greater than that of the waterjet.

4. RANGE gives the program user a choice of four possible engines for propulsion and lift. The program contains specific fuel consumption (SFC) data on each engine and feeds it into a Breguet range equation. The range equation is exercised through 10 increments of total SES weights; each increment is based on a 10-percent burnoff of fuel from the previous increment. At each selected speed, a new drag is calculated for each new weight, resulting in a different NPC and SFC.

The previous four subroutines are part of SESPAR. The subsequent examples and figures show results of this computer prediction program.

Fig. 24 is a plot of drag versus velocity for four different High L/B SES displacements (5600, 6400, 7200, and 8000 tons). In actuality it is the same ship with four different fuel loads. Also shown on the plot are three different waterjet

*SESPAR was developed with funds from the Surface Effect Ship Project Office, Naval Sea Systems Command, PMS-304.

**The capability also exists to use the wavemaking drag theory of Ref. 5.

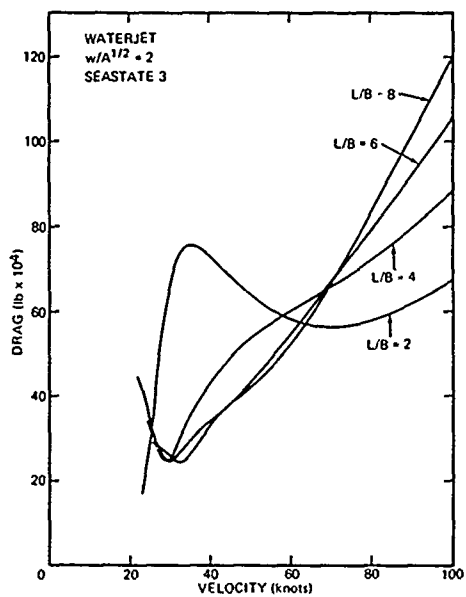


Fig. 22a - 6,000 Ton SES

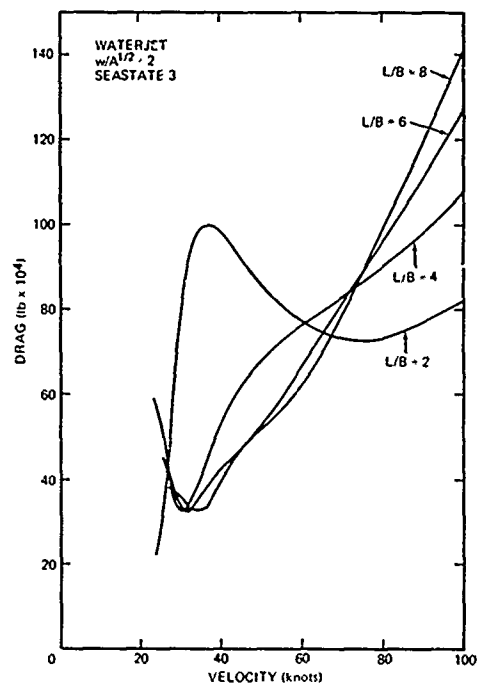


Fig. 22b - 8,000 Ton SES

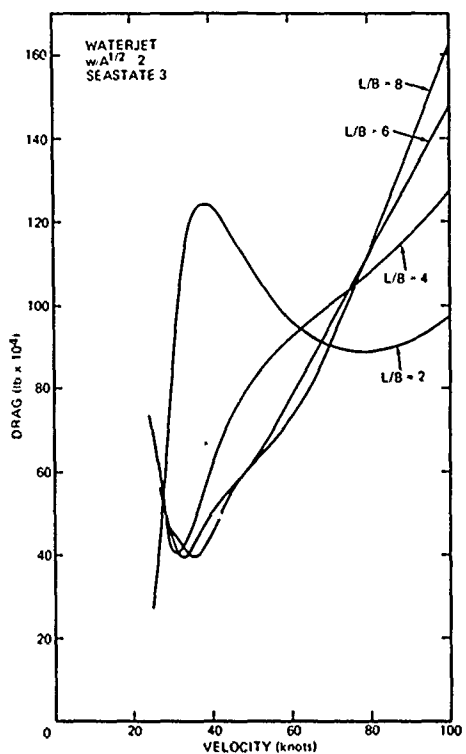


Fig. 22c - 10,000 Ton SES

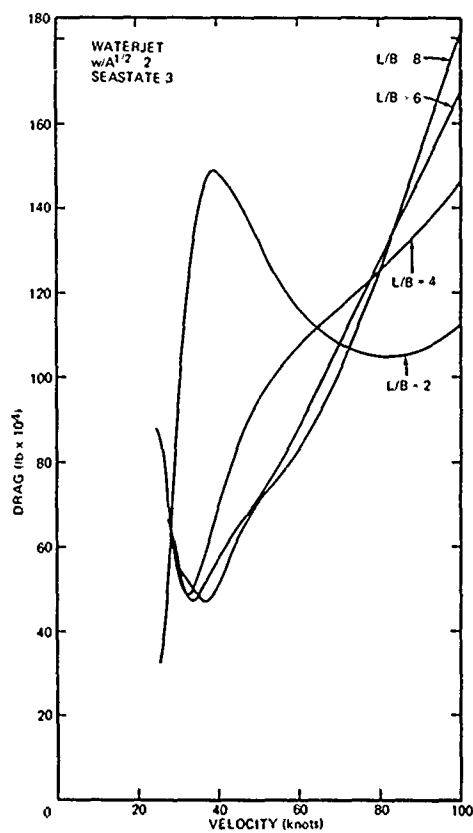


Fig. 22d - 12,000 Ton SES

Figure 22 - Drag versus Velocity for Four Displacements and Four L/B Values

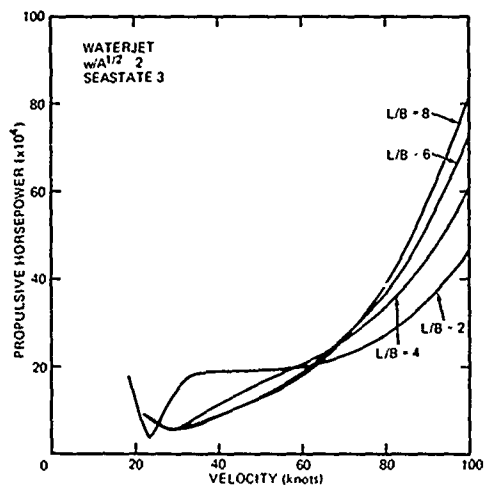


Fig. 23a - 6,000 Ton SES

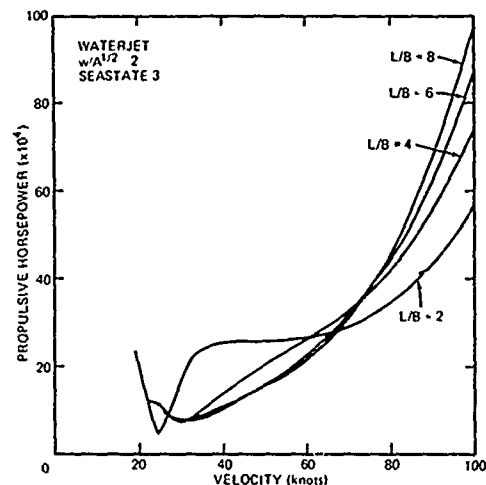


Fig. 23b - 8,000 Ton SES

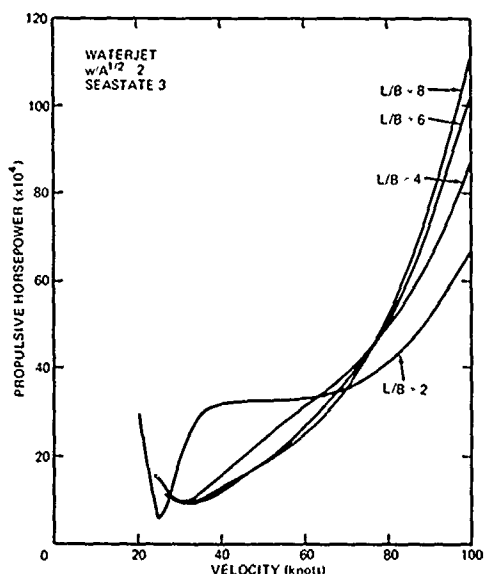


Fig. 23c - 10,000 Ton SES

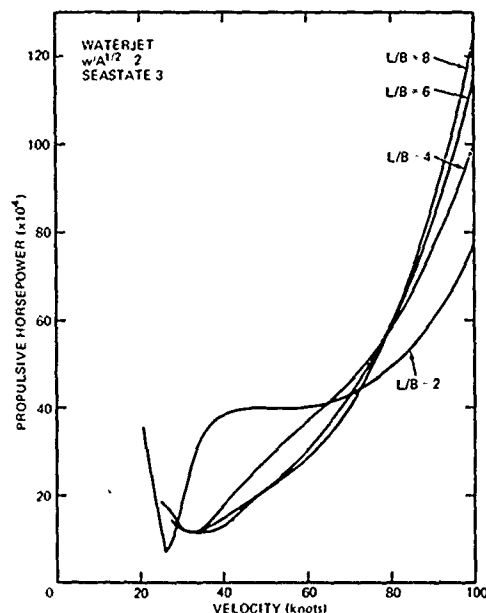


Fig. 23d - 12,000 Ton SES

Figure 23 - Power versus Velocity for Four Displacements and Four L/B Values

thrust available lines associated with three different installed propulsive power levels. For each thrust available line it is seen what speed improvement can be achieved as ship load is decreased or conversely what speed penalty will be realized as the ship is overloaded. For example, the thrust available line for a 150,000 hp waterjet propulsion system intersects the drag curve for the 8000 ton high L/B at 53.3 knots. Then, as fuel burns off, the speed capability increases until the SES weighs 5600 tons and its drag curve is intersected by the same thrust available line at 67.5 knots.

An important conclusion from Fig. 24 is that the velocity degradations are modest with increases in the fuel load (or payload), and further that the tradeoff between increased fuel load (or payload)

and velocity degradation is available as a design option. For example, a 25 percent fuel addition, and the resultant substantial range increase, would be at the expense of the modest decrease in speed associated with about a 10 percent increase in displacement. Note that for even the substantial increase in displacement from 5600 to 8000 tons, the secondary hump drag does not cause any radical velocity drop by exceeding the thrust available. The importance of this conclusion cannot be overstated, particularly in an advanced vehicle type for which there can be substantial risk in the certainty of a given weight estimate. An unexpected increase in SES lightship weight then results in only a modest velocity degradation and not a loss of fuel load (and hence range) or payload. The choice of a minor velocity degradation versus the alternatives may be a more acceptable solution.

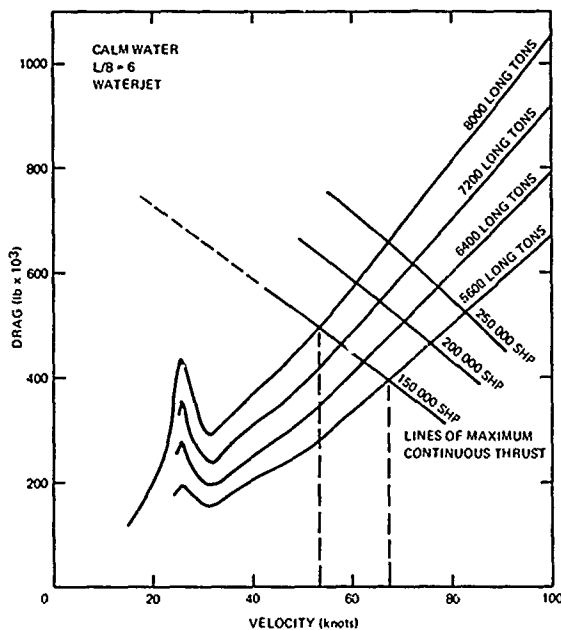


Fig. 24 - Performance Plot Showing Speed Capability for Various Fuel Loadings as a Function of Thrust

Fig. 25 is a plot of drag versus velocity for an 8000 ton SES with $L/B = 6$ and $w/A^{1/2} = 2$. It shows the drag in calm water and in States 3, 4, and 5 seas. A waterjet thrust available line is also added so that the velocity degradation can be seen. The velocity degradation in a State 5 sea does not appear to be a serious limitation for the 8000 ton SES. However, it should be noted that the magnitude of the degradation increases as the SES displacement decreases.

Fig. 26 is a plot of drag versus velocity for two 8000 ton SES's with the same cushion area and pressure, but with different length-to-beam ratios. One vehicle is a Low L/B SES ($L/B = 2$), and the other is a High L/B SES ($L/B = 6$). The L/B 6 SES does not have the large hump which is characteristic of the L/B 2 SES and thus the L/B 6 SES is free to operate in the 30- to 60-knot regime and can operate there with a significantly reduced propulsive horsepower. Also, note here that the secondary wavemaking drag hump (at approximately 20 knots for the L/B 2 curve) can usually be lowered experimentally to a magnitude less than the primary hump value.

Fig. 27 is a plot of effective horsepower versus velocity for an L/B 2 SES and an L/B 6 SES. Both have the same cushion area and displacement (8000 tons).

Fig. 28 is similar to Fig. 27 except that propulsive shaft horsepower (rather than effective horsepower) is plotted on the ordinate. Included on the figure are three data points which are representative of three current Navy ships. Both Figs. 27 and 28 illustrate the lesser horsepower requirement for the high L/B as contrasted with the low L/B in the 15- to 60-knot regime. Also from Fig. 28 it is shown that the High L/B SES requires less propulsive power than the 7300 ton

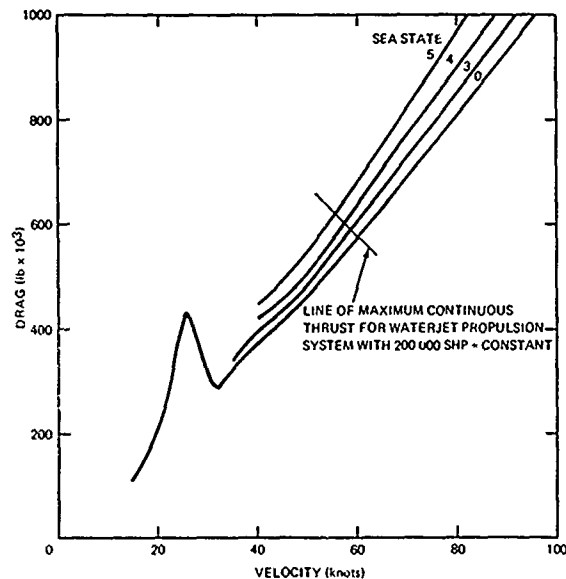


Fig. 25 - Sea State Degradation for an 8,000 ton, L/B 6.0 SES

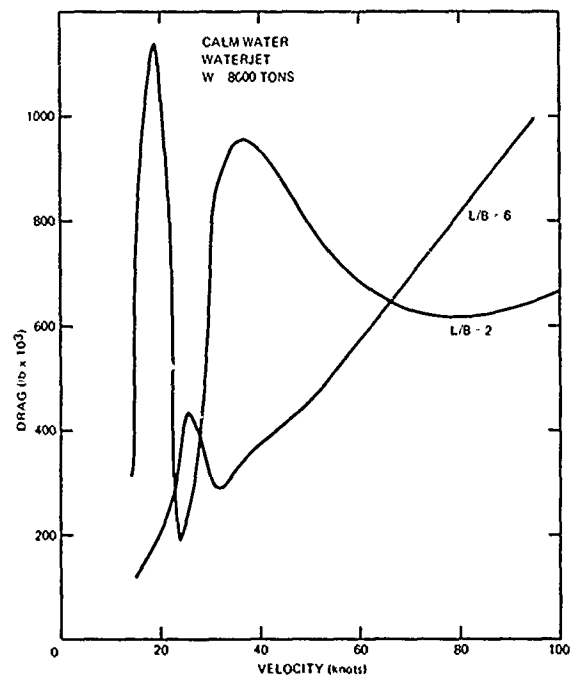


Fig. 26 - Total Drag versus Velocity Comparison for L/B 2.0 and 6.0

Spruance Class Destroyer at approximately 30 knots even though the total installed power is about the same. In addition, the High L/B SES compares favorably with the other two classes of ships considering that they are less than half its displacement. The important conclusion here is not that the High L/B SES compares favorably with conventional displacement hulls near 30 knots, but rather that it is capable of a better job in the 40- to 60-knot speed regime.

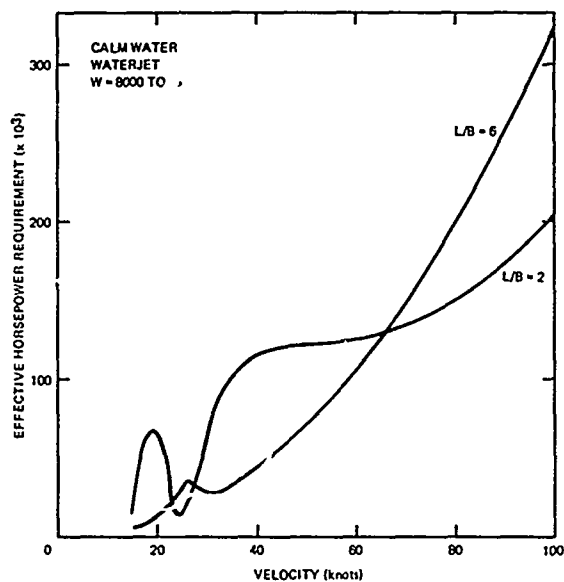


Fig. 27 - Effective Horsepower versus Velocity for L/B 2.0 and 6.0

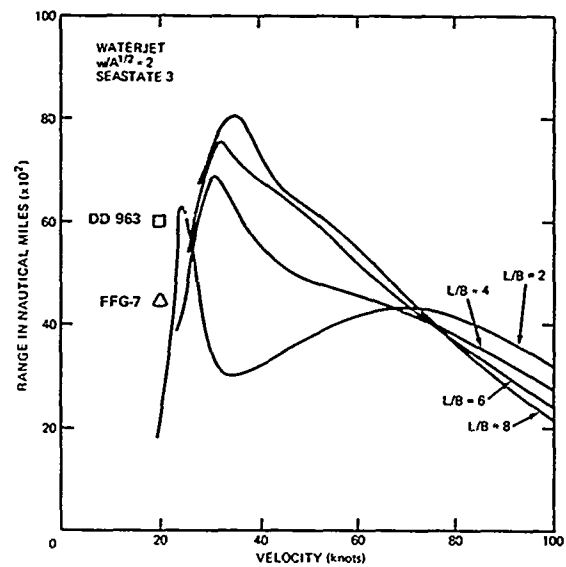


Fig. 29 - Range versus Velocity as a Function of L/B

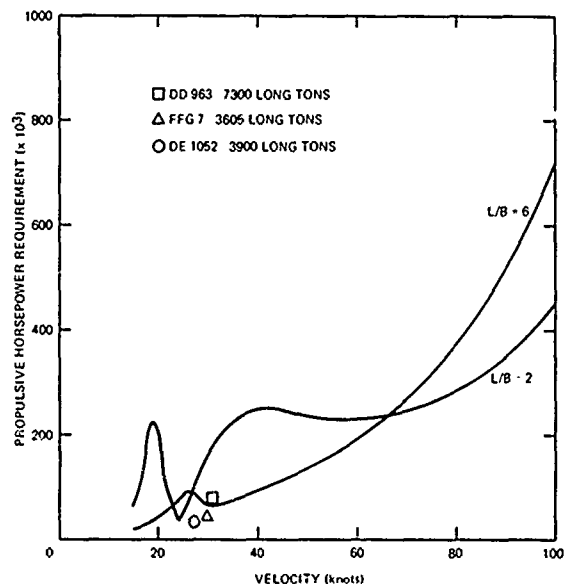


Fig. 28 - Propulsive Horsepower Requirements for L/B 2.0 and 6.0 8,000 Ton SES Compared with Conventional Displacement Ships

Fig. 29 is a plot of range versus velocity for four 8000 ton SES's, all with the same cushion area, but with different L/B values (L/B = 2, 4, 6, and 8). These ships are all waterjet propelled. Conclusions, which can be drawn from Fig. 29, are listed below:

1. In excess of 70 knots, the Low L/B SES (L/B = 2) achieves the greatest ranges.
2. Below 65 knots, the higher L/B SES's achieve the greatest ranges.

3. Below 70 knots the ranges of the Low L/B SES decrease with decreasing speed.

4. Below 70 knots the ranges of the higher L/B SES's increase with decreasing speed down to about 35 knots. In other words, ranges can be increased by slowing down. This is a substantial advantage from a design point of view as well as from an operational point of view.

5. With such high SES ranges in the 30-60 knot regime, the High L/B SES is an economical craft to operate even at the speeds of our conventional Navy ships (e.g., 30 knots). Included on the plot are two data points which allow comparison of ranges of the High L/B SES with the range of the DD-963 and the FFG-7.⁶

Other design requirements are not so easily addressed, but they can be indirectly assessed. For example: (1) A plot of propulsive shaft horsepower is a good indicator of cost, (2) Comparison studies showing the transport efficiency versus velocity of one ship type with others is another method of selecting the most economical to operate. (3) Selection of ship design based on the highest payload-to-power ratio is another indicator for ships of equal speed. (4) Comparison of the rates of fuel consumption at a given speed and displacement is a measure of how economical a ship is to operate. These points are each discussed subsequently.

Fig. 30 (nearly identical to Fig. 28 except for scale) is a plot of propulsive shaft horsepower per ton displacement versus velocity for a High L/B 8000 ton SES. Included on this plot are the DD-963, FFG-7, and DE-1052 points.⁶ With these points normalized in this fashion, the SES compares very favorably with these new classes of conventional ships. This particular plot shows the SES with a slight advantage, however lift power was not included. With lift power included the SES curve would lay right on the DD-963 and FFG-7 data points.

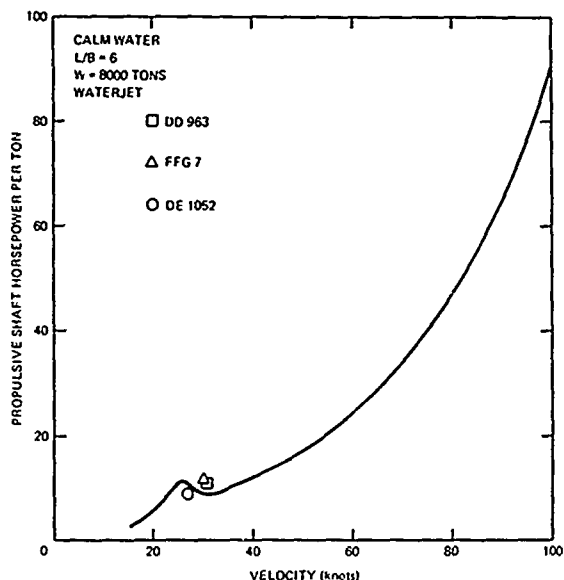


Fig. 30 - Propulsive Shaft Horsepower per Ton versus Velocity for a High L/B SES

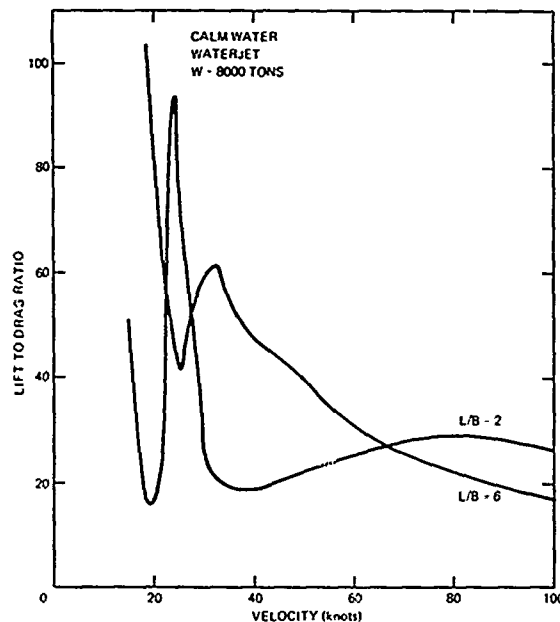


Fig. 32 - Lift-to-Drag Ratio for L/B 2.0 and 6.0

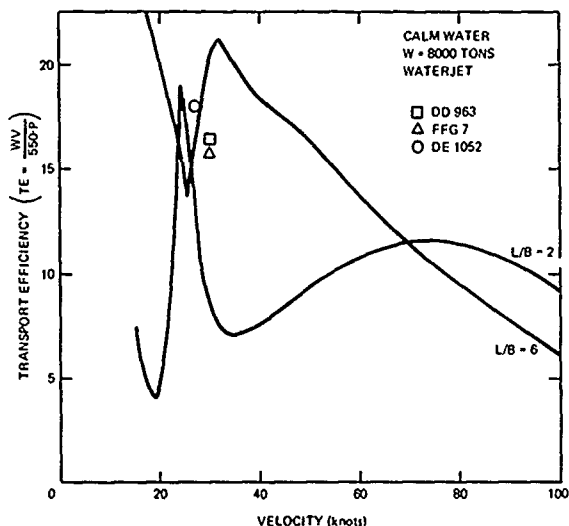


Fig. 31 - Transport Efficiency versus Velocity for L/B 2.0 and 6.0

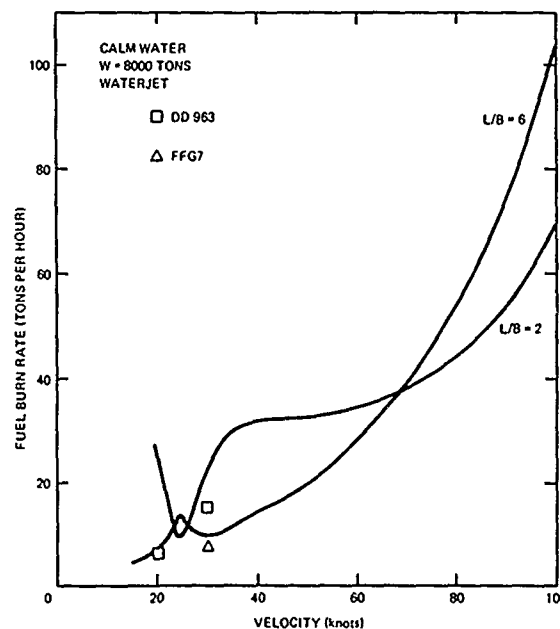


Fig. 33 - Fuel Burn Rate versus Velocity for L/B 2.0 and 6.0

Fig. 31 is a plot of transport efficiency versus velocity for both a High and Low L/B 8000 ton SES.⁸ Transport efficiency is by definition equal to the product of the weight and velocity divided by the total power. This plot is very similar to that of range versus velocity, Fig. 29. Data points for the DD-963, FFG-7, and DE-1052 class ships are also included on this plot.⁶

Fig. 32 is a plot of lift-to-drag ratio versus velocity. It also follows the same trends as that of Fig. 29.

Fig. 33 is a plot of fuel burn rate (FBR) versus velocity for the High and Low L/B 8000 ton SES's. The trend is as expected. Below the crossover point (at 68 knots) the high L/B has

significantly lower fuel burn rates, while the low L/B is better above. In the 28+ knot region, the high L/B may actually have lower burn rates than many of our older Navy vessels. In fact from the literature⁹ there was enough information to couple with known engine data to calculate fuel burn rates for two vessels now in production, the Spruance Class Destroyer and the Perry Class Frigate. The two calculated points are shown on the plot. The high L/B FBR is 33 percent lower than that of the 7300 ton DD-963 and 25 percent higher than the 3600 ton FFG-7 at 30 knots.

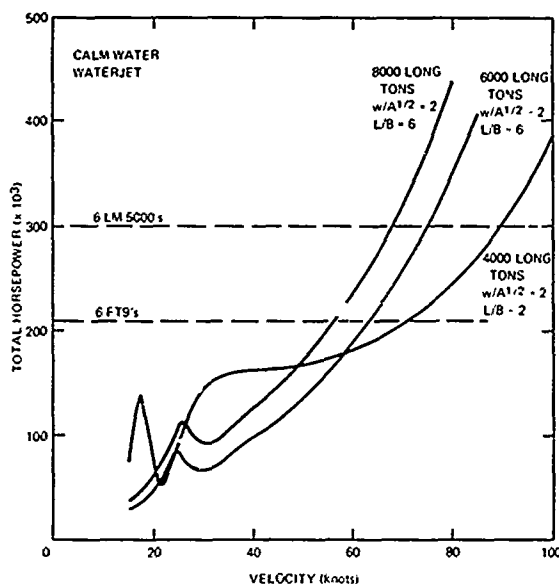


Fig. 34 - Total Horsepower versus Velocity Illustrating SES Design Options

Fig. 34 is a plot of total horsepower requirement versus velocity for three SES's: (1) a 4000 ton SES with $w/A^{1/2} = 2$ and $L/B = 2$, (2) a 6000 ton SES with $w/A^{1/2} = 2$ and $L/B = 6$, and (3) an 8000 ton SES with $w/A^{1/2} = 2$ and $L/B = 6$. Table 1 lists the maximum velocities for each of two powering configurations, (6 FT9's and 6 LM5000's). It also lists ranges obtainable and payloads that were included in the calculations.

The most important point to be made from Table 1 is that the 8000 ton High L/B SES has a much greater payload carrying capability for the same installed power plant. The only penalty associated with its usage is about a 20 percent speed degradation. Neglecting any other advantages the decision to carry double the payload as opposed to a 20 percent speed degradation is a choice which would be based on the merit of speed versus range and payload in the Navy missions for which the design is being considered.

It is obvious, looking at these families of surface effect ships, that the High L/B SES is a very attractive concept. It offers high speed (relative to conventional displacement ships), a broad operating speed capability (15-60 knot), high ranges, a stable platform, and a large potential for growth in displacement. The high L/B is weight sensitive, but not volume limited. The low L/B has to be concerned with adequate thrust for required hump margin and this represents a limitation on displacement growth for any specific propulsion plant design. Since a large drag hump does not exist for the high L/B, the only limitation exists in the form of a hard requirement on the maximum speed. The High L/B SES actually has potential for a large amount of growth in its gross displacement. It was shown in Fig. 34 and Table 1 that an 8000 ton High L/B SES could be driven at 68 knots by waterjet

Table 1 - SES Powering Characteristics

	Displacement long tons		
	4000	6000	8000
L/B	2	6	6
$w/A^{1/2}$	2	2	2
V_{max}^*	71 knots	63 knots	56.5 knots
V_{max}^{**}	89 knots	75 knots	68 knots
Range†	3180 n.mi.	4200 n.mi.	5200 n.mi.
Range††	3680 n.mi.	5400 n.mi.	5960 n.mi.
Payload	400 tons	600 tons	800 tons

*Velocity obtainable with a 6 FT9's

**Velocity obtainable with 6 LM5000's

†Ranges all calculated at maximum velocity with 6 LM5000's supplying the propulsion and lift requirement.

††Ranges calculated at 60 knots with 6 LM5000's.

propulsion with the same propulsion plant that propels a 4000 ton Low L/B SES at 89 knots. Similarly, it is shown in Fig. 28 that the high L/B requires no more propulsive power to drive than comparable size conventional ships with gas turbine propulsion plants at equivalent speeds in the 20-30 knot range.

But in spite of an approximate thrust power equality near 30 knots, the design velocity selected for the High L/B SES would probably be much higher than that of the DD-963 or FFG-7, because substantial speed increases are possible with reasonable power increases. From Fig. 34, a total power of 175,000 hp, with waterjet propulsion, would yield a design speed of 50 knots for an 8000 ton High L/B SES. It would take twice this power to attain 75 knots in an 8000 ton L/B 2 SES.

The foregoing powering information is of added significance when projected vehicle costs are approximated by the method of Dix and Riddell.⁷ This method, according to these authors, "adequately meets the goal of evaluating a vehicle concept's economics long before hardware development."⁷ They conclude that "for vehicles with large power/weight ratios that are not mass produced (a description which fits practically all military vehicles), cost* is directly proportional to installed power."⁷ If this approximate costing method is accepted, then it can be concluded that a 50 knot High L/B SES would be about 50 percent of the cost of a high-speed (75 knot) L/B 2 SES of equal displacement. In any case, it should be substantially less expensive, even if Ref. 7 is not totally relied on.

*"Vehicle cost means the procurement cost of the bare vehicle without payload. In combat vehicles all offensive and defensive armament must be considered payload."⁷

A final point to be made in contrasting the High L/B SES with a conventional ship is that current Navy vessels have a requirement to add ballast as fuel is spent to maintain the design metacentric height, whereas both High and Low L/B SES's enjoy the speed increase which results from decreased ship weight as fuel is burned.

Summary

The High L/B SES differs from any other SES only in the respect that the ratio of its length to its beam is large (e.g., 5 to 7). Its total drags are lower than those of lower L/B SES's up to a crossover speed; hence speeds less than crossover are natural design speeds for the High L/B SES. Crossover speeds increase with displacement (60 knots at 5,000 tons, 68 knots at 10,000 tons), and High L/B SES designs are considered most applicable to these larger displacements for Navy missions where large payloads are required.

A substantial experimental program has been conducted at DTNSRDC from the early 1970s to the present. Model powering and motion tests were performed in calm water and seas with SES models with various L/B values, and a suitable range of other significant parameters. Stability tests and analyses were also conducted. A High L/B SES manned experimental craft, the XR-5, was then built and successfully operated in drag, motion, maneuvering, and structural trials.

The foregoing experimental data correlate well with an SES parametrics computer prediction program, which in turn, is used to arrive at realistic initial SES designs. Using results from this program, drag and powering data are displayed as a function of speed, L/B, displacement, and other significant parameters. From this information important conclusions can be drawn, as follows:

1. As fuel burns for any SES the speed capability increases, because burned fuel need not be replaced by water ballast.
2. Velocity degradations for the High L/B SES are modest with increases in displacement, and this is available as an important design option.
3. The High L/B SES can operate in the 30- to 60-knot regime with a relatively low installed power.
4. An 8000 ton High L/B SES, with a speed of about 50 knots, has a power advantage of about a factor of 2 when compared with a 75 knot L/B 2 SES of equal displacement. Based on an approximate costing model,⁷ in which cost and power are closely correlated, it also has a substantial cost advantage.
5. Of the competing forms of propulsion, the semi-submerged supercavitating propeller appears to have a potential for achieving net propulsive coefficients about 25 percent higher than those of waterjets.

6. The velocity degradation in high seas does not appear to be a serious limitation for large High L/B SES's (5,000 to 10,000 tons), but this degradation increases as the SES displacement decreases.

7. Although the High L/B SES designs compare favorably with other classes of ships near 30 knots, the principal point is that they are significantly better in the 40- to 60-knot speed regime.

8. The achievable ranges (and also transport efficiencies, and lift-to-drag ratios) of the High L/B SES, in the 30- to 60-knot speed regime, improve significantly with decreased speed.

In an overall view of SES design, it can be concluded that the SES principle applies very broadly, to ships of very high speed (Low L/B SES), and to ships of moderately high speed (High L/B SES). In fact a tradeoff exists between speed and displacement for a given level of installed power.

References

1. Ford, A.G., "Captured Air Bubble (CAB) Vehicle Progress Report," Paper No. 67-348 presented at the First AIAA/SNAME Advance Marine Vehicles Meeting, Norfolk, Virginia (May 1967). Also Journal of Hydronautics, Vol. 2, No. 2, pp 81-86 (Apr 1968).
2. Eggington, W.J. and N. Kobitz, "The Domain of the Surface-Effect Ship," Paper No. 11 presented at SNAME Annual Meeting, New York, N.Y. (Nov 1975).
3. Fee, J.J. and E.H. Handler, "U.S. Navy SES Program," Paper No. 76-856 presented at the AIAA/SNAME 3rd Advanced Marine Vehicles Conference, Arlington, Virginia (Sep 1976).
4. Newman, J.N. and F.A.P. Poole, "The Wave Resistance of a Moving Pressure Distribution in a Canal," DTNSRDC Report 1619 (Mar 1962). Also Schiffstechnik (Hamburg), Vol. 9 (Jan 1962).
5. Doctors, L.J. and S.D. Sharma, "The Wave Resistance of an Air-Cushion Vehicle in Steady and Accelerated Motion," Journal of Ship Research, Vol. 16, No. 4, pp. 248-260 (Dec 1972).
6. Jane's Fighting Ships, Jane's Yearbooks, London, England, pp. 598-605 (1977-1978).
7. Dix, D.M. and F.R. Riddell, "Projecting Cost-Performance Trade-offs for Military Vehicles," Astronautics and Aeronautics, pp. 40-50 (Sep 1976).
8. von Karman, T. and T.G. Gabrielli, "What Price Speed?" Mechanical Engineering, pp. 775-781 (Oct 1950).

INITIAL DISTRIBUTION

Copies

1 ARPA/Library
 1 CHONR/461
 1 ONR SCI LIAISON GP/APO
 1 NAV STRATEGIC SYS PROJ
 OFFICE
 PM-1
 1 USNA/Library
 2 NAVPGSCOL
 1 Library
 1 D. Layton/Aero Dept
 1 NROTC & NAVADMINU, MIT
 1 NSWC/Dahlgren
 Tech Library
 1 NSWC/White Oak
 Tech Library
 1 NUSC/Tech Library
 19 NAVSEA
 1 SEA 03B
 1 SEA 032
 1 SEA 09G32
 16 PMS-304-141
 1 NISC
 3 NAVSEC
 1 SEC 6110
 1 SEC 6114
 1 SEC 6136
 12 DDC
 1 Coast Guard HQ
 Library/5-2

Copies

1 Marine Corps HQ/AX
 A.L. Slafkosky/Sci
 Advisor
 2 Maritime Admin
 1 R&D Office
 1 Div of Ship Design
 1 Library of Congress
 Science & Tech Div
 1 AIAA/D. Staiger
 1 SIT/Davidson Lab
 J.P. Breslin

CENTER DISTRIBUTION

Copies

Copies	Code	Name
10	5214.1	Reports Distribution
1	522.1	Library (C)
1	522.2	Library (A)
1	522.3	Aerodynamics Library

DTNSRDC ISSUES THREE TYPES OF REPORTS

1. DTNSRDC REPORTS, A FORMAL SERIES, CONTAIN INFORMATION OF PERMANENT TECHNICAL VALUE. THEY CARRY A CONSECUTIVE NUMERICAL IDENTIFICATION REGARDLESS OF THEIR CLASSIFICATION OR THE ORIGINATING DEPARTMENT.

2. DEPARTMENTAL REPORTS, A SEMIFORMAL SERIES, CONTAIN INFORMATION OF A PRELIMINARY, TEMPORARY, OR PROPRIETARY NATURE OR OF LIMITED INTEREST OR SIGNIFICANCE. THEY CARRY A DEPARTMENTAL ALPHANUMERICAL IDENTIFICATION.

3. TECHNICAL MEMORANDA, AN INFORMAL SERIES, CONTAIN TECHNICAL DOCUMENTATION OF LIMITED USE AND INTEREST. THEY ARE PRIMARILY WORKING PAPERS INTENDED FOR INTERNAL USE. THEY CARRY AN IDENTIFYING NUMBER WHICH INDICATES THEIR TYPE AND THE NUMERICAL CODE OF THE ORIGINATING DEPARTMENT. ANY DISTRIBUTION OUTSIDE DTNSRDC MUST BE APPROVED BY THE HEAD OF THE ORIGINATING DEPARTMENT ON A CASE-BY-CASE BASIS.